Biophysical Chemistry 23 (1985) 139–145
Elsevier

BPC 01033

TEMPERATURE DEPENDENCE OF ANION TRANSPORT INHIBITOR BINDING TO HUMAN RED CELL MEMBRANES

Richard G. POSNER and James A. DIX

Department of Chemistry, State University of New York, Binghamton, NY 13901, U.S.A.

Received 20th June 1985
Accepted 2nd September 1985

Key words: Red cell membrane; Thermodynamics; Anion transport; Band 3; 4,4'-Dibenzamido-2,2'-disulfonic stilbene

The binding characteristics of the inhibitor of anion transport in human red cells, 4,4'-dibenzamido-2,2'-disulfonic stilbene (DBDS), to the anion transport protein of red cell ghost membranes in buffer containing 150 mM NaCl have been measured over the temperature range 0–30°C by equilibrium and stopped-flow fluorescence methods. The equilibrium dissociation constant, K_{eq}, increased with temperature. No evidence of a 'break' in the $\ln(K_{eq})$ vs. $1/T$ plot was found. The standard dissociation enthalpy and entropy changes calculated from the temperature dependence are 9.1 ± 0.9 kcal/mol and 3.2 ± 0.3 e.u., respectively. Stopped-flow kinetic studies resolve the overall binding into two steps: a bimolecular association of DBDS with the anion transport protein, followed by a unimolecular rearrangement of the DBDS-protein complex. The rate constants for the individual steps in the binding mechanism can be determined from an analysis of the concentration dependence of the binding time course. Arrhenius plots of the rate constants showed no evidence of a break. Activation energies for the individual steps in the binding mechanism are 11.6 ± 0.9 kcal/mol (bimolecular, forward step), 17 ± 2 kcal/mol (bimolecular, reverse step), 6.4 ± 2.3 kcal/mol (unimolecular, forward step), and 10.6 ± 1.9 kcal/mol (unimolecular, reverse step). Our results indicate that there is an appreciable enthalpic energy barrier for the bimolecular association of DBDS with the transport protein, and appreciable enthalpic and entropic barriers for the unimolecular rearrangement of the DBDS-protein complex.

1. Introduction

Temperature dependences of equilibrium and kinetic processes in biological systems can be used to calculate equilibrium and activation thermodynamic parameters. Although the interpretation of these parameters cannot be as precise as that in a more well-defined physico-chemical system, the thermodynamic parameters nonetheless give an approximation of the energies of the equilibrium states of the biological system and of the activation barriers connecting the equilibrium states.

In addition to giving energy levels, temperature dependences often reveal 'breaks' in plots of the logarithm of the equilibrium or rate constant vs. inverse absolute temperature. Breaks are usually interpreted as phase changes in the biological system [1], or as competition between two opposing processes [2].

We have measured the equilibrium and rate constants that characterize the binding of a fluorescent inhibitor of red cell anion transport, 4,4'-dibenzamido-2,2'-disulfonic stilbene (DBDS), to human red cell ghost membranes over the temperature range 0–30°C. DBDS binds specifically to band 3, the anion transport protein of the red cell membrane [3]; the binding is accompanied by a 100-fold increase in the quantum yield of fluorescence. In the presence of chloride, the binding mechanism of DBDS to band 3 consists of a bimolecular association of DBDS with band 3, followed by a unimolecular rearrangement of the

DBDS-band 3 complex:

$$\text{band 3} \underset{k_{-1}}{\overset{k_1}{\rightleftharpoons}} \text{band 3-DBDS} \underset{k_{-2}}{\overset{k_2}{\rightleftharpoons}} \text{band 3*DBDS} \quad (1)$$

$$\text{DBDS}$$

in which k_i and k_{-i} are the forward and reverse rate constants, respectively, of the i-th step [4]. Both steps can be resolved kinetically by stopped-flow fluorescence experiments [5].

Studies of a variety of red cell membrane properties, including anion transport [6], glucose transport [7], water transport [8], and membrane lipid viscosity [9], have revealed breaks in Arrhenius plots in the temperature range 10–20°C. We do not find breaks in Arrhenius plots for DBDS equilibrium and kinetic constants. The bimolecular step in DBDS binding is characterized by a large activation enthalpy, much larger than would be expected for a simple diffusion-controlled bimolecular association. The unimolecular step is characterized by large enthalpic and entropic barriers, as would be expected for a DBDS-induced conformational change in the band 3 protein.

2. Materials and methods

2.1. Membrane preparations

Human red cell ghost membranes were prepared from outdated blood obtained from the Red Cross Blood Bank. The blood was washed 3 times in 20 vols. of 150 mM NaCl, 5 mM sodium phosphate, pH at 8, 0°C, then hemolyzed at 0°C with 20 vols. of 5 mM sodium phosphate, pH 8. Hemolysate was removed by washing four times with 20 vols. of 5 mM sodium phosphate, pH 8. The ghost membranes were then washed twice with 20 vols. of 150 mM NaCl, 5 mM Hepes, pH 7.4; this buffer was used in the subsequent experiments. Ghost membranes were suspended to 0.04 mg total protein/ml; protein concentration was measured according to the method of Lowry et al. [16].

2.2. Equilibrium experiments

Equilibrium DBDS fluorescence was measured in an SLM 4000 fluorescence spectrometer equipped with a double excitation monochrometer and cooled photomultiplier. The spectrometer was interfaced with a Digital MINC 11/23 computer (Maynard, MA) for data averaging, storage and analysis. 3 ml of a 0.04 mg/ml ghost solution were tritrated with concentrated stock solutions of DBDS; final DBDS concentrations ranged from 0.02 to 14 μM. The resulting fluorescence was corrected for dilution, scattering and fluorescence of unbound DBDS as described by Verkman et al. [3]. The corrected fluorescence was analyzed in terms of a single class of DBDS-binding sites. The temperature was maintained by circulating temperature-controlled water through the SLM cuvette holder block; temperature was measured by immersing a thermometer into the cuvette after completion of the experiment.

2.3. Kinetic measurements

The kinetics of DBDS binding to band 3 were measured by fluorescence stopped-flow methods. 0.1 ml of a 0.04 mg/ml ghost solution (approx. 100 nM band 3) was mixed with 0.1 ml of a DBDS solution of known concentration in a Dionex Model D-130 stopped-flow photometer (Sunnyvale, CA) interfaced with a Digital MINC 11/23 computer for data acquisition and analysis. Typically, four to six scans at a given DBDS concentration and temperature were averaged before analysis. The temperature of the reaction was maintained by circulating temperature-controlled water through a water bath containing the mixing syringes and mixing block, and through the block containing the observation cell. A double-exponential function was fitted through the averaged data by the nonlinear least-squares method; rate constants were extracted from the exponential time constants of the fit as described in section 3.2 and as described by Smith and Dix [5].

3. Results and discussion

3.1. Equilibrium studies

The effect of temperature on DBDS equilibrium binding to red cell ghost membranes is

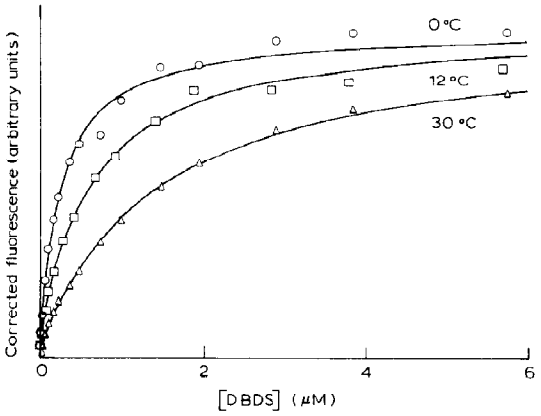

Fig. 1. Effect of temperature on DBDS equilibrium binding to ghost membranes. The ordinate is fluorescence of DBDS, corrected for dilution, scattering and unbound DBDS [3]; the abscissa is total DBDS concentration. The lines are the nonlinear least-squares fit of a rectangular hyperbola, $F = e_1[\mathrm{DBDS}]/(K_{eq} + [\mathrm{DBDS}]) + e_2$, where F is the corrected fluorescence and e_1, K_{eq} and e_2 fitted parameters. The data have been normalized to corrected fluorescence intensity at infinite [DBDS] in order to take into account the variation of quantum yield with temperature. (○) 0°C, (□) 12°C, (△) 30°C.

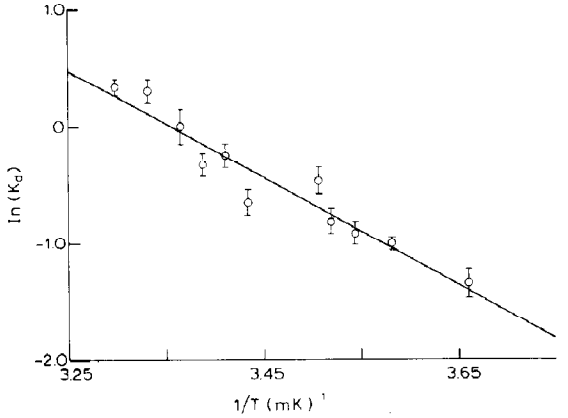

Fig. 2. Effect of temperature on equilibrium DBDS dissociation constant. The logarithm of the dissociation constant, K_{eq}, determined from the fit of a rectangular hyperbola to binding data as in fig. 1, is plotted as a function of inverse absolute temperature. The line is the weighted least-squares fit.

shown in fig. 1. The overall dissociation constant for DBDS binding, K_{eq}, is obtained from fig. 1 as the concentration of DBDS at which the corrected fluorescence half-saturates. K_{eq} is related to the rate constants of the DBDS binding mechanism in eq. 1 by

$$K_{eq} = (k_{-1}/k_1)/(1 + k_2/k_{-2}) \qquad (2)$$

As shown in fig. 1, the dissociation constant increases with temperature, corresponding to a total negative enthalpy change accompanying DBDS binding.

A value for the overall enthalpy and entropy changes is calculated from the equation relating the equilibrium constant to temperature:

$$\ln(K_{eq}) = -\Delta H/RT + \Delta S/R \qquad (3)$$

A plot of $\ln(K_{eq})$ vs. $1/T$ is given in fig. 2; the standard enthalpy and entropy changes calculated from the slope and intercept are given in the first line of table 1. The data in fig. 2 fall along a straight line and do not exhibit a significant break, suggesting that DBDS binding to band 3 is not sensitive to any phase changes that might occur in the membrane over this temperature range, or that DBDS binding does not consist of two competing processes with differing temperature dependences.

3.2. Kinetic studies

The effect of temperature on the rate of DBDS binding is shown in fig. 3. As temperature increases, the rate of binding increases. The time course of binding is not single exponential but double exponential [5], reflecting contributions from each of the two steps in the binding mechanism of eq. 1.

For [DBDS] ≫ [band 3] (which is applicable in our experiments), the time course of DBDS binding is described by two coupled differential equations; in matrix form, these equations are [5]:

$$\begin{pmatrix} -\mathrm{d}x/\mathrm{d}t \\ -\mathrm{d}y/\mathrm{d}t \end{pmatrix} = \begin{pmatrix} k_1[\mathrm{DBDS}] + k_{-1} & k_{-1} \\ k_2 & k_2 + k_{-2} \end{pmatrix} \begin{pmatrix} x \\ y \end{pmatrix} \qquad (4)$$

where x and y represent deviations of [band 3] and [band 3*-DBDS], respectively, from their equilibrium values. The solution to eq. 4 is of the form

$$x + y = A_1 \exp(-t/\tau_1) + A_2 \exp(-t/\tau_2) \qquad (5)$$

Table 1

Standard thermodynamic parameters characterizing DBDS binding at 25°C

Standard state: 1 M, activity coefficients = 1.

Parameter	Value	Units	ΔH (kcal/mol)	ΔS (cal/mol per K)	ΔG (kcal/mol)	E_a (kcal/mol)
K_{eq}	0.77	μM	9.1 ± 0.9	3.21 ± 0.3	8.2 ± 0.5	–
k_1	0.67	$s^{-1}\,\mu M^{-1}$	11.0 ± 0.9	6.6 ± 0.7	9.0 ± 1.2	11.6 ± 0.9
k_{-1}	2.4	s^{-1}	17 ± 2	−0.45 ± 0.07	17 ± 2	17 ± 2
k_2	1.31	s^{-1}	5.7 ± 2.3	−35 ± 18	16 ± 8	6.4 ± 2.3
k_{-2}	0.52	s^{-1}	10.0 ± 1.9	−26 ± 7	18 ± 4	10.6 ± 1.9
From Verkman et al. [3]						
k_2	4.0	s^{-1}	5.3 ± 1.6	−38 ± 9	17 ± 6	–
k_{-2}	0.09	s^{-1}	12.2 ± 2.4	−24 ± 3	19 ± 6	–

where τ_1^{-1} and τ_2^{-1} are the eigenvalues of the rate constant matrix in eq. 4 and A_1 and A_2 are related to the eigenvectors of the equation. The quantity $x + y$ is related to the measured quantity in our kinetic experiments, [band 3-DBDS] + [band 3*-DBDS]. If the quantum yield of DBDS fluorescence is the same in both the band 3-DBDS and band 3*-DBDS forms, then $x + y$ is just proportional to [band 3-DBDS] + [band 3*-DBDS]; if one form fluoresces more than the other, then the eigenvectors will be affected but the eigenvalues will remain relatively unaffected.

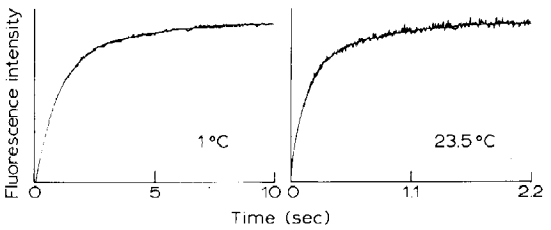

Fig. 3. Effect of temperature on time course of DBDS binding to ghost membranes. Equal volumes of ghost membranes (0.04 mg/ml) and DBDS (10 μM) were mixed in a stopped-flow device and the resulting fluorescence followed as a function of time. The data shown in this figure represent the average of four time courses. Increasing fluorescence represents formation of the band 3-DBDS and band 3*-DBDS species in the mechanism of eq. 1 in the text. The lines are a fit of a double-exponential function to the data. (Left) 1°C, fast time constant = 1.23 ± 0.02 s, slow time constant = 3.3 ± 0.3 s; (right) 23.5°C, fast time constant = 0.11 ± 0.01 s, slow time constant = 0.59 ± 0.04 s.

The time constants, τ_1 and τ_2, were determined at a given temperature for five DBDS concentrations in the range 5–15 μM, by a fit of a double-exponential function to each time course. Theoretical time constants, predicted by solving the rate matrix for a given [DBDS] and assumed rate constants, were compared to the time constants obtained from the double-exponential fit. The rate constants were then varied until the deviation between the calculated time constants and the experimental time constants was minimized. In order to minimize the number of variable parameters, the combination of the four rate constants k_1, k_{-1}, k_2 and k_{-2} was constrained to equal the equilibrium dissociation constant as calculated by eq. 2 at the appropriate temperature.

Fig. 4 shows the temperature dependence of the rate constants, plotted in the form of an Arrhenius plot. None of the four rate constants exhibits a significant break in the Arrhenius plot, suggesting that even on a mechanistic level, as given in eq. 1, there are no thermal transitions as probed by DBDS binding.

We have used Eyring activated-complex theory to calculate the thermodynamic parameters characterizing the kinetics of DBDS binding. The Arrhenius plot of the temperature dependence of a rate constant, k_i, yields an activation energy, E_a

$$\ln(k_i) = -E_a/RT + \ln(A) \qquad (6)$$

where A is the Arrhenius frequency factor. The standard activation enthalpy change, $\Delta H^{\ddagger}$, is

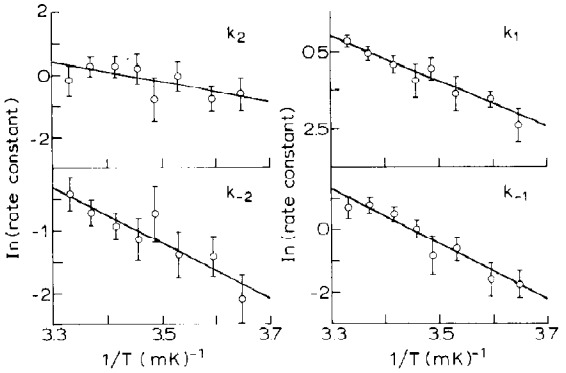

Fig. 4. Arrhenius plots of rate constants for DBDS binding to ghost membranes. Forward and reverse rate constants for the individual steps in the DBDS-binding mechanism of eq. 1 were extracted from the concentration dependence of the fitted time constants as described in the text. The lines represent the weighted least-squares fit. (Left, top) forward unimolecular step, (left, bottom) reverse unimolecular step, (right, top) forward bimolecular step, (right, bottom) reverse bimolecular step.

calculated from E_a as

$$\Delta H^{\ddagger} = E_a - RT \tag{7}$$

and the standard activation entropy change, $\Delta S^{\ddagger}$, for a given temperature, T, is calculated as

$$\Delta S^{\ddagger} = R\left(\ln(k_i) + \Delta H^{\ddagger} - \ln(k_B T/h)\right) \tag{8}$$

where k_B is Boltzmann's constant and h Planck's constant [10]. The standard activation enthalpies and entropies are given in table 1.

3.3. Thermodynamic profile

The activation parameters can be combined to give a thermodynamic profile for DBDS binding to band 3 (fig. 5). At 25°C, the bimolecular step of the reaction mechanism is both enthalpy ($\Delta H = -6$ kcal/mol) and entropy ($-T\Delta S = -1.8$ kcal/mol) driven, resulting in a favorable free energy change ($\Delta G = -7.6$ kcal/mol). The major activation barrier for the bimolecular step is enthalpic. For the unimolecular step, a favorable enthalpy change ($\Delta H = -4.3$ kcal/mol) is opposed by an unfavorable entropy change ($-T\Delta S = +2.6$ kcal/mol), resulting in a small, favorable free energy change ($\Delta G = -1.7$ kcal/mol). The

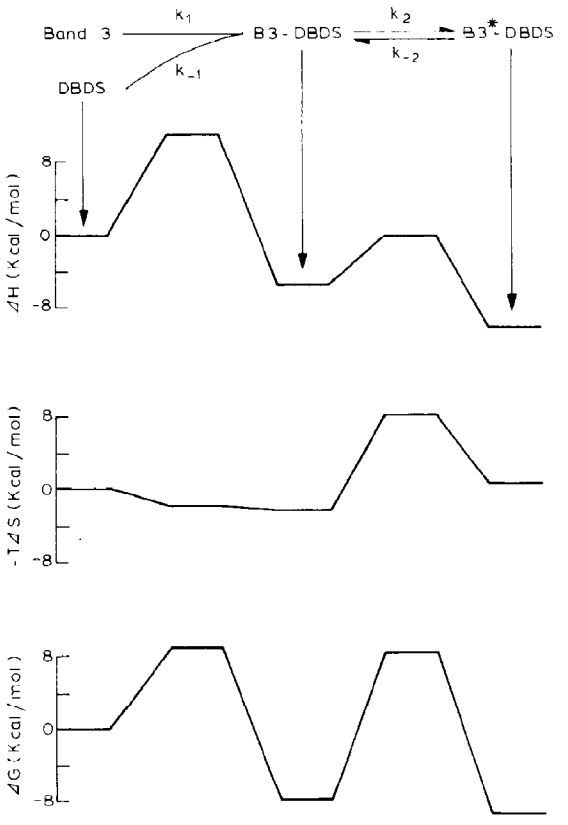

Fig. 5. Thermodynamic profile for DBDS binding to ghost membranes at 25°C.

major activation barriers for the unimolecular step are both enthalpic and entropic. Similar thermodynamic profiles have been observed for enzyme reactions [11].

Consideration of the thermodynamic parameters of fig. 5 leads a plausible molecular model for DBDS binding. The binding site for DBDS on band 3 may be a narrow cavity to which DBDS has restricted diffusional access. In order for DBDS to associate with this binding site, enthalpic bonds must be broken (large, positive activation enthalpy) and the protein must adopt a slightly more disordered state (positive entropy of activation); this would correspond to opening up to make it more accessible to DBDS. Once DBDS has bound to this site, additional enthalpic bonds must be broken and the protein must adopt a much more

ordered state (large negative activation entropy) in order for DBDS to bind to its final, band 3*-DBDS form; this would correspond to an internalization of the DBDS molecule within the band 3 protein.

3.4. Comparison with previous work

Verkman et al. [3] have studied the thermodynamics of DBDS binding to ghost membranes suspended in sodium citrate buffer, 160 mM ionic strength, rather than the chloride buffer used in the present study. In buffers that do not contain transportable anions, such as citrate buffer, DBDS binds to two classes of band 3 sites on ghost membranes. Because of the large dead time of their stopped-flow apparatus, Verkman et al. were not able to detect fast, bimolecular steps in binding. In spite of the differences between our experimental conditions and those of Verkman et al., the thermodynamic profiles for the unimolecular step of binding are remarkably similar (table 1), suggesting that the energy barriers for the rearrangement and the equilibrium states of the band 3-DBDS complex do not depend strongly on the presence of transportable anions.

In the present study, and in the study of Verkman et al. [3], Arrhenius plots of rate constants were linear and did not reveal any characteristic break. This finding is in contrast with breaks determined from log plots of red cell membrane parameters vs. inverse absolute temperature. Such plots reveal a thermal transition in the temperature range 10–20°C. A summary of reported transition temperatures is given in table 2.

Table 2

Reported transition temperatures in the red cell membrane

System	Method	T_c(°C)	Reference
Intact cells	water transport	26	[8]
	glucose exchange	20	[7]
	glucose efflux	none	[13]
	chloride exchange	15	[6]
	bromide exchange	25	[6]
	NBD-taurine efflux	10	[12]
Ghost membranes	positron lifetime	16–20	[14]
Sonicated ghosts	viscometry	18–19	[9]
Sonicated lipids	viscometry	18–19	[9]
Intact cells	bicarbonate exchange	12–24	[15]

It is perhaps surprising that there is no evidence of a break in the Arrhenius plots of the binding rate constants of DBDS to band 3, while Arrhenius plots of rate constants for anion transport through band 3 reveal breaks [6,12]. However, anion transport involves at least two steps, an anion-binding step and an anion translocation step; if these two steps have different activation energies, then measurement of just the overall exchange rate as a function of temperature could lead to apparent breaks as the temperature dependence of one step dominates the temperature dependence of the other [2,12].

In our binding studies, we are able to resolve the individual steps in the binding mechanism, thereby determining the activation barriers for each individual step. We have used our results to analyze the effect of temperature on a two-step binding mechanism if the kinetic data were fitted incorrectly by a single-exponential time course. Simulated time courses for the reaction mechanism in eq. 1 were calculated from the rate equations in eq. 4 and the rate constants for a particular temperature as obtained from the fitted lines in fig. 4. The simulated time courses were then fitted by a single-exponential function from 200 ms to 4-times the fitted time constant; over this time range, the simulated data were described reasonably well by the single-exponential fitting function.

If a single-exponential function is fitted to the simulated data, then a break in the Arrhenius plot of the log of the inverse fitted exponential time constant vs. reciprocal absolute temperature is seen at 19°C, similar to the temperature at which a break in the Arrhenius plot of chloride exchange flux is observed [6]. These results indicate that if a two-step mechanism were fitted incorrectly to a single-step mechanism, then an apparent break in an Arrhenius plot could be observed. If, in our studies, we probe the overall state of band 3, then our data suggest that breaks in Arrhenius plots of anion exchange data result from competition between the temperature dependences of anion-binding and/or anion translocation steps, and not from a phase change in the transport protein or surrounding lipid.

Acknowledgements

We thank Mr. Kevin Smith for stimulating discussions, Ms. Patty Rumola for ghost preparation, and Ms. Karen McNamara for assistance. This work was supported by NIH grant R01 HL29488.

References

1 L. Thilo, H. Trauble and P. Overath, Biochemistry 16 (1977) 1283.
2 J.R. Silvius and R.N. McElhaney, J. Theor. Biol. 88 (1981) 135.
3 A.S. Verkman, J.A. Dix and A.K. Solomon, J. Gen. Physiol. 81 (1983) 421.
4 J.A. Dix, A.S. Verkman and A.K. Solomon, J. Membrane Biol. (1986) in the press.
5 K.R. Smith and J.A. Dix, (1985) submitted.
6 J. Brahm, J. Gen. Physiol. 70 (1977) 283.
7 L. Lacko, B. Wittke and P. Geck, J. Cell. Physiol. 82 (1973) 213.
8 V.V. Morariu, V.I. Pop, O. Popescu and G. Benga, J. Membrane Biol. 61 (1981) 1.
9 G. Zimmer and H. Schirmer, Biochim. Biophys. Acta 345 (1974) 314.
10 R.S. Berry, S.A. Rice and J. Ross, Physical Chemistry (Wiley, New York, 1980).
11 K.J. Laidler and B.F. Peterman, Methods Enzymol. 63 (1979) 234.
12 O. Eidelman and Z.I. Cabantchik, J. Membrane Biol. 71 (1983) 141.
13 A.K. Sen and W.F. Widdas, J. Physiol. 160 (1962) 392.
14 E.I.-H. Chow, S.Y. Chuang and P.K. Tseng, Biochim. Biophys. Acta 646 (1981) 356.
15 E.I.-H. Chow, E.D. Crandall and R.E. Forster, J. Gen. Physiol. 68 (1976) 633.
16 O.H. Lowry, N.J. Rosebrough, A.L. Farr, and R.J. Randall, J. Biol. Chem. 193 (1951) 265.